Regularities of Angular Distribution of Near-Horizon Sky Brightness in the Cloudless Atmosphere

S.M. Sakerin, T.B. Zhuravleva, and I.M. Nasrtdinov
Institute of Atomospheric Optics SB RAS
Tomsk, Russia

Introduction

The methods of sun-photometry of the atmosphere based, for example, on interpretation of the angular distribution of radiation in the solar almucantar are widely used for retrieval of the aerosol optical characteristics (Dubovik et al. 2000). Preliminary analysis has shown that the near-horizon region also can be interesting for solving some applied problems. As is known, investigations of the structure of the daytime cloudless sky brightness at observation from the ground were carried out principally at zenith angles less than 80° in visible wavelength range. For further development of the methods it is necessary to obtain more complete data on the distribution of the cloudless sky brightness at great zenith angles of observation and wider wavelength range. The regularities of formation of the sky brightness field in the near-horizon region and just above the horizon line are considered in this paper.

The Method for Numerical Modeling

To calculate the fields of the incoming solar radiation, we have developed an effective algorithm for statistical modeling (method of conjugated trajectories), which allows to take into account: (a) sphericity of the atmosphere, (b) scattering and absorption in the aerosol-gas atmosphere, (c) vertical inhomogeneity of the atmosphere, and (d) reflection from the underlying surface. The vertically inhomogeneous model of the aerosol-gas atmosphere is specified as a set of homogeneous layers, each characterized by the aerosol extinction and scattering coefficients, molecular scattering coefficient, and absorption coefficient, as well as the aerosol $g_A(\theta)$ and Rayleigh $g_R(\theta)$ scattering phase functions. The incident radiation is reflected from the surface according to the Lambert law with the albedo A_S. Molecular absorption is taken into consideration through expansion of the wide-band transmission function into exponential series (k-distribution method). The transmission functions are calculated using the HITRAN-2000 database of spectroscopic data with the allowance made for the spectral apparatus functions typical for filter sun photometers (Chesnokova et al. 2003). The calculations of the effective molecular absorption coefficients involve the vertical profiles of pressure, temperature, and gas concentrations, corresponding to the AFGL “mid-latitude summer” model (Anderson et al. 1986); the optical characteristics of aerosol are chosen in accordance with the WCP recommendations (WCP 1986) for the continental conditions. Vertical stratification of the aerosol extinction coefficient in the majority of the presented calculations was set in the form of exponential distribution. The input parameters varied within the following ranges: aerosol optical depth $0.05 \le \tau_A \le 0.3$; surface albedo $0.0 \le A_S \le 0.7$; solar zenith angle $0 \le SZA \le 88$ and viewing zenith angle $85 \le$ viewing zenith angle (VZA) ≤ 90.

The numerical model of the brightness field of the cloudless sky near the horizon is developed on the basis of the described algorithm. Main regularities of formation of the daytime cloudless sky brightness and the factors, which determine them, are revealed by means of this model.

Dependence of the Near-Horizon Sky Brightness on the Aerosol Optical Thickness

According to the theory of radiation transfer in the atmosphere, two factors affect the dependence of the diffuse radiation on the horizon B_H on τ_A. On the one hand, the increase of the aerosol optical thickness means the increase of the number of scatterers, and, hence, favors the increase of brightness. On the other hand, the increase of τ_A leads to more significant extinction of radiations reaching an elementary scattering volume, and, hence, favors the decrease of the diffuse radiation. Competitions of these two contrary factors can be the reason of deviation of the dependence of the sky brightness on the aerosol optical thickness from monotonous.

The presence and position of the sky brightness maximum as function of τ_A (at fixed other parameters of the atmosphere) also depends on φ and SZA. The brightness $B_H(\tau_A)$ at azimuth angles of observation $\varphi<90°$ has the well pronounced maximum, the position of which moves to the range of less values τ_A as SZA increases (Figure 1). As the azimuth increases ($\varphi>90°$), $B_H(\tau_A)$ is transformed to the monotonously decreasing function of τ_A. Analysis of the results shows that the near-horizon sky brightness at great zenith angles of the Sun SZA≥75° and τ_A≥0.05 decreases with increase of τ_A in the whole range of the angles of observation $0\leq\varphi\leq180°$. Let us note that non-monotonous manner of the dependence of the brightness BH(τA) is determined, first of all, by its single component $B_{0,H}(\tau_A)$; the behavior of the multiple component $B_{m,H}(\tau_A)$ is qualitatively analogous, but its maximum is less pronounced and is shifted to the side of greater values τ_A.

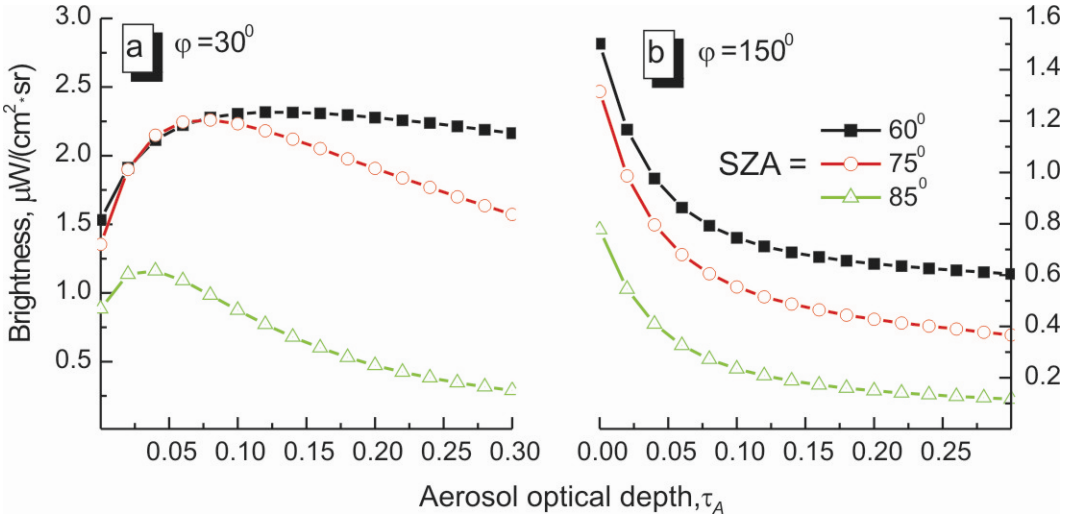

Figure 1. The near-horizon brightness as function of the aerosol optical thickness for two azimuth angles of the detector at different zenith angles of the Sun.

The Dependence of B_H on the Aerosol Single Scattering Albedo

The results of numerical modeling show that the effect of the aerosol single scattering albedo (SSA) in the atmospheric layers h>2 km on the near-horizon sky brightness $B_H(\varphi)$ is ignorable: the relative differences in calculations at variations 0.85<SSA<1 do not exceed 2%. SSA significantly affects $B_H(\varphi)$ in more dense near-ground layer h<2 km.

To understand the mechanism of the effect of SSA on $B_H(\varphi)$, let us use the single scattering approximation in the plane-parallel geometry:

$$B_{0,H} = I_0\, g_{atm}(\theta)\exp[-(\tau_A+\tau_R)m]; \quad g_{atm}(\theta) = (\tau_A\, g_{atm}(\theta)\, SSA + \tau_R\, g_{atm}(\theta))/(\tau_A+\tau_R).$$

The scattering angle θ and the azimuth angle φ are related here by the formula $\cos\theta = \cos(VZA)\cdot\cos(SZA)+\sin(VZA)\cdot\sin(SZA)\cdot\cos\varphi$, $m \approx 1/\cos(SZA)$. For convenience of the description, azimuth distributions of the sky brightness $B_H(\varphi)$ are represented in the form of dependences on the scattering angles $B_H(\theta)$.

The dependence of $B_H(\theta)$ and its single $B_{0,H}(\theta)$ and multiple $B_{m,H}(\theta)$ components on SSA in the typical range of the values 0.85<SSA<1, τ_A=0.2 and SZA=75° is close to linear (Figure 2). Aerosol has prevalent effect on the value $B_{0,H}(\theta)$ in the forward direction (φ<60°) due to the strong asymmetry of $g_A(\theta)$. The change of SSA to 15% leads to the same relative change of $B_{0,H}(\theta)$ (~15%). The role of molecular scattering increases in the short-wave range at great azimuths (φ>90°), and the effect of SSA on the component $B_{0,H}(\theta)$ weakens (10%). More essential dependence of the multiple component of brightness on SSA is observed due to the increase of the number of "scattering-absorption" acts: variations of $B_{m,H}(\theta)$ as function of φ comprise 30-35%.the increase of the aerosol absorption ability in the noted limits is accompanied by the decrease of the sky brightness $B_H(\theta)$ by 25-30%. Variations of the brightness $B_H(\theta)$ as function of SSA show weak dependence on SZA.

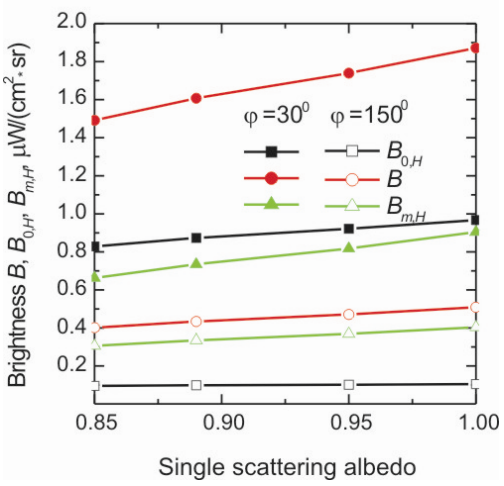

Figure 2. The brightness $B_H(\varphi)$, $B_{0,H}(\varphi)$, $B_{m,H}(\varphi)$ as function of the aerosol single scattering albedo at τ_A=0.2 and SZA=75° and the azimuth angles of the receiver φ =30° and φ =150°.

Azimuth Dependence of B_H

The peculiarities of the angular structure of the diffuse radiation $B_H(\varphi)$ is regulated by redistribution of the role of both the aerosol $g_A(\theta)$ and molecular $g_R(\theta)$ scattering phase functions and multiple $B_{m,H}(\varphi)$ and single $B_{0,H}(\varphi)$ scattering.

As is known, aerosol scatters radiation mainly in the forward hemisphere: the asymmetry factor $G = \int_0^{\pi/2} g(\theta(\sin\theta in \Big/ \int_{\pi/2}^{\pi} g(\theta(\sin\theta in$ of molecular scattering is equal to 1, while that of aerosol is essentially greater, $G_A \approx 3–11$. Thus, the effect of aerosol implies in increase of the anisotropy of the sky brightness, and the effect of molecular scattering is contrary (Figure 3a).

The principal peculiarity of the angular distribution is significant increase of the scattered radiation at $\varphi \rightarrow \varphi_{Sun}$ due to strong asymmetry of $g_A(\theta)$ and fulfillment of the condition $\tau_A \geq \tau_R$ (in the greatest part of the considered wavelength range). As moving from the Sun, the effect of $g_R(\theta)$ becomes more essential, and the contribution of multiple scattering increases. Due to this fact, the sky brightness phase function becomes more flat (Figure 3b). The point of redistribution of the contribution of aerosol and molecular scattering is in the range $\theta \approx 60°$. In the case when the optical thickness τ_R has become comparable with τ_A (visible range), molecular scattering phase function $g_R(\theta)$ mainly affects the diffuse radiation in the back hemisphere.

Transformation of the angular dependence $B_H(\theta)$ with the wavelength λ (Figure 3) is the consequence of the dependence of $g_{atm}(\theta)$ on the relative value τ_A/τ_R. As $\tau_R \sim \lambda^{-4}$, and $\tau_A \sim \lambda^{-1}$, the increase of the wavelength leads to redistribution of the role of the components of scattering: the atmospheric scattering phase function approaches to aerosol ($g_{atm} \rightarrow g_A$), the fraction of single scattering increases, and the sky brightness phase function becomes more elongated. Molecular scattering in the wavelength range $\lambda > 1\mu m$ becomes less significant, $g_{atm}(\theta) \approx g_A(\theta)$ and the sky brightness in the whole range of the scattering angles is determined mainly by aerosol characteristics τ_A and $g_A(\theta)$.

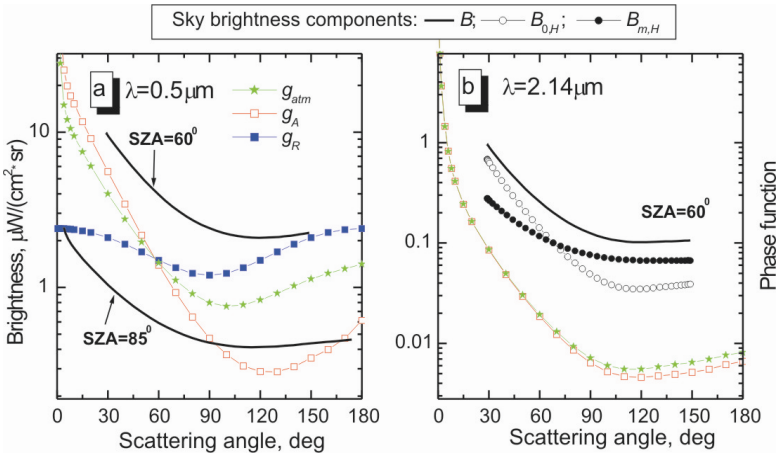

Figure 3. Azimuth distributions of the near-horizon sky brightness; (a) at zenith angles of SZA = 60 and 85° (τ_A=0.2); (b) the brightness components $B_{0,H}$ and $B_{m,H}$ separately (τ_A=0.1). The scattering phase functions g_{atm}, g_A and g_R are also presented here.

Dependence of the Sky Brightness on the Viewing Zenith Angle

Dependence of the scattered radiation on increasing of VZA is determined by (a) the increase of brightness with the increase of the scattering volume (the number of particles) along the direction of vision; (b) the decrease of brightness due to the increase of extinction of radiation illuminating the atmospheric column; (c) the decrease ($\theta<90°$) or the increase ($\theta>90°$) of brightness with the increase of the scattering angle θ due to the increase of the angle |SZA–VZA|. The effect of the "Phase function" factor (c) prevails only in the range of solar aureole, where the most elongated part of the scattering phase function $g_A(\theta)$ has been realized.

The main tendency out of the near-Sun region is the increase of the scattered radiation B(VZA) with the increase of the zenith angle of observation VZA (Figure 4a). The angular dependence in the near-horizon area are divided into to types: 1) monotonous manner is kept right up to crossing the horizon line; 2) non-monotonous behavior of B(VZA) with the maximum in the range VZA>80° and subsequent decrease of brightness to the horizon. The non-monotonous behavior of B(VZA) observed at approaching to horizon (VZA$\rightarrow$90°) is determined by redistribution of the aforementioned factors.

The sky brightness has minimum values under conditions of high atmospheric transparency ($\tau_A\rightarrow0$) and sharply increases only near the horizon. When the transparency has decreased (τ_A =0.1), the total level of brightness increases, and a narrow maximum B_{max}(VZA*) appears near the horizon. When the aerosol optical thickness has decreases still more (τ_A =0.2), the brightness maximum moves from the horizon, becomes wider, and its value begins to decrease. At the same time, the sky brightness in the region VZA<VZA* continues to increase with increase of τ_A. Such a behavior of B(VZA) in the near-horizon region is formed under the effect of the comparable contribution and qualitatively analogous dependence of the components of single and multiple scattering on VZA (Figure 4b). The changes of the values of albedo of the underlying surface A_S and single scattering SSA weakly affect the manner of the zenith distribution of the sky brightness near the horizon.

The peculiarities of the angular behavior B(VZA) in different wavelength ranges are determined by the spectral dependence of the optical thickness $\tau(\lambda) = \tau_A(\lambda) + \tau_R(\lambda)$. The value $\tau(\lambda)$ in visible and UV wavelength ranges, as a rule, is not less than 0.2–0.3, so the maximum B_{max}(VZA*) covers the quite wide angular range and the decrease of brightness to the horizon begins from VZA≈80°. In IR range, due to quick decrease of τ_R and then τ_A, angular position of the brightness maximum moves to the horizon and takes the final value VZA*=90°.

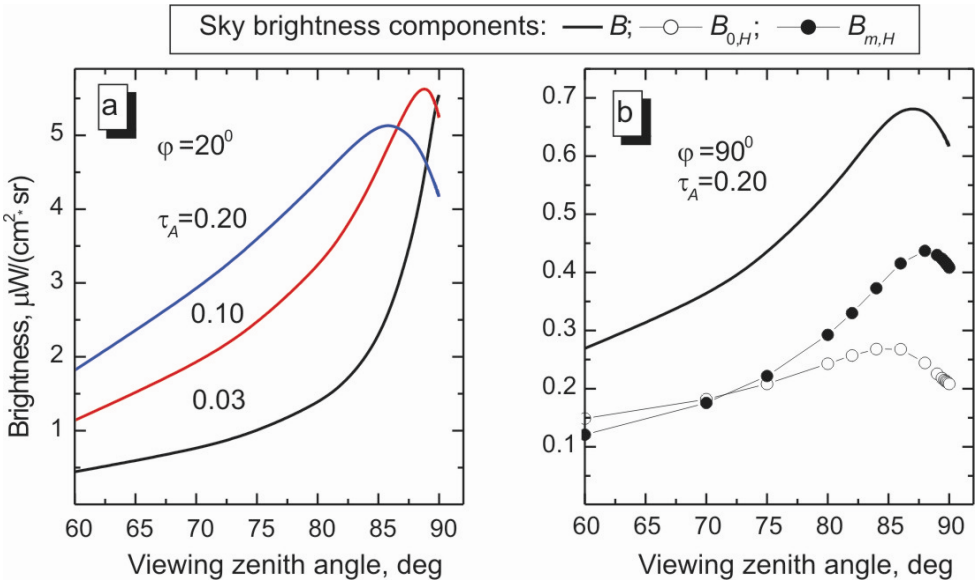

Figure 4. Sky brightness as function of viewing zenith angle (λ=0.87 μm): (a) at different values τ_A; (b) the brightness components $B_{0,H}$ and $B_{m,H}$ separately (τ_A=0.2). SZA=75°.

Comparison of the Results of Numerical Modeling with the Experiment

A field experiment was carried out in summer 2003. It was aimed at the study of angular distributions of the incoming diffuse radiation in the near-horizon sky region. The experiment was carried out in the forest zone ("Background" field site of IAO SB RAS) 60 km far from Tomsk and included three types of measurements; (a) sky brightness in the solar almucantar (SZA=VZA); (b) azimuth distribution of the sky brightness in the near-horizon region (80 – 89°); and (c) the dependence of the sky brightness on the zenith angle of observation. The scanning photometer capable of measuring in the wavelength range 0.44 to 1.06 μm and the sun photometer for accompanying measurements of the aerosol optical thickness in the range 0.37 to 1.06 μm were used in the experiment.

The measured values τ_A were used as input parameters at numerical modeling, and the other parameters ($g_A(\theta)$, A_S, SSA, etc.) were set according to the models mentioned in the beginning of the paper. The results of calculations and measurements of the brightness fields are shown in Figures 5 and 6. The considered effect of the "horizon getting dark" (the decrease of brightness at the range VZA*–90°) is confirmed by the experiment (Figure 6). Besides, this figure illustrates, how the brightness maximum B_{max}(VZA*) transforms with the wavelength.

The results of numerical and field experiments are in good agreement. It allows us to suppose that the selected model is adequate and can be used for description of the brightness fields near the horizon.

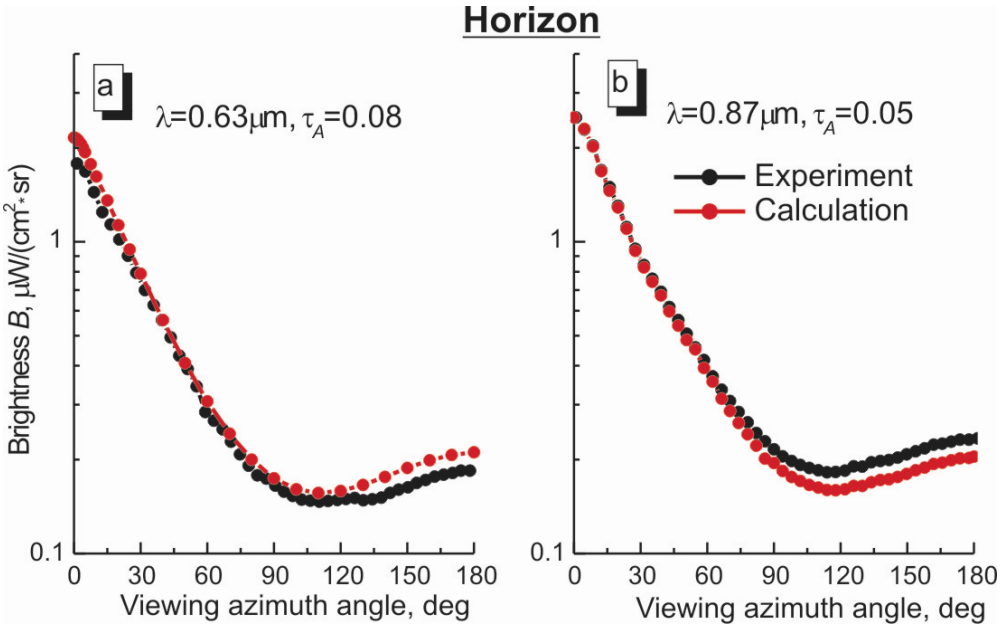

Figure 5. Model and measured near-horizon sky brightness fields. (a) λ=0.63 μm and (b) λ=0.87 μm. (SZA=82°, VZA=87°, A_S=0.2).

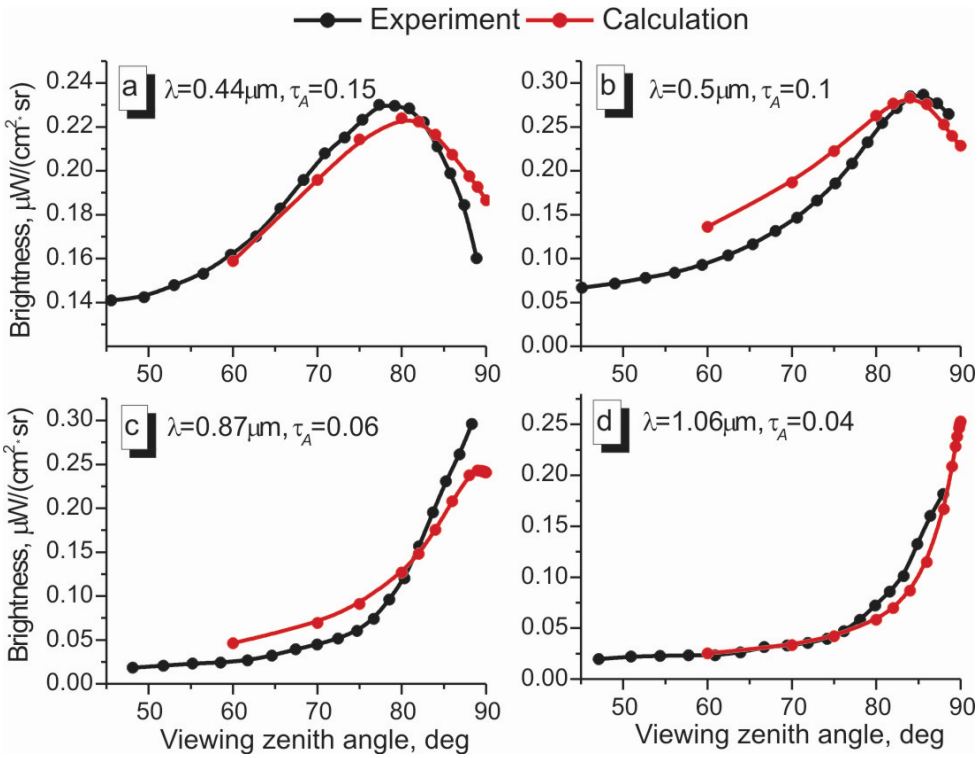

Figure 6. Model and measured near-horizon sky brightness fields as functions of zenith angle of observation (SZA=56°, φ=150°, A_S=0.2).

Contact

S.M. Sakerin

Acknowledgment

This work was supported, in part, by the U.S. Department of Energy's ARM Program (contract No. 5012).

References

Anderson, G, S Clough, F Kneizys, J Chetwynd, and E Shettle. 1986. AFGL Atmospheric Constituent Profiles (0-120 km). Air Force Geophysics Laboratory. AFGL-TR-86-0110, Environmental Research Paper No. 954.

Chesnokova, TY, KM Firsov, IM Nasrtdinov, SM Sakerin, VV Veretennikov, and TB Zhuravleva. 2003. In *Proceedings 13-th ARM Science Team Meeting*. March 31-April 4, 2003, Broomsfield, CO. http://www.arm.gov/publications/proceedings/conf13/extended_abs/chesnokova-tyu.pdf

Dubovik, OT, and M King. 2000. "A flexible inversion algorithm for retrieval aerosol optical properties from Sun and sky radiance measurements." *Journal of Geophysical Research* 105(D16):20,673-20,696.

World Climate Research Programme (WCP). 1986. A preliminary cloudless standard atmosphere for radiation computation. WCP-112, WMO/TD N 24, p 60.